

# Supramolecular Structure of the Mitochondrial Oxidative Phosphorylation System\*

Published, JBC Papers in Press, November 13, 2006, DOI 10.1074/jbc.R600031200

Egbert J. Boekema<sup>‡</sup> and Hans-Peter Braun<sup>§1</sup>

From the <sup>‡</sup>Groningen Biomolecular Sciences and Biotechnology Institute, University of Groningen, Nijenborgh 4, 9747 AG Groningen, The Netherlands and the <sup>§</sup>Institute for Plant Genetics, Faculty of Natural Sciences, Universität Hannover, Herrenhäuser Strasse 2, 30419 Hannover, Germany

**The protein complexes of the mitochondrial oxidative phosphorylation system were recently reported to form supramolecular assemblies termed respiratory supercomplexes or respirasomes. These supercomplexes are considered to be of great functional importance. Here we review new insights into supercomplex structure and physiology.**

The oxidative phosphorylation (OXPHOS)<sup>2</sup> system forms the basis for mitochondrial ATP production. In most organisms it is composed of the ATP synthase complex (complex V) and four oxidoreductase complexes: the NADH dehydrogenase (complex I), the succinate dehydrogenase (complex II), the cytochrome *c* reductase (complex III), and the cytochrome *c* oxidase (complex IV). All these complexes reside within the inner mitochondrial membrane. Complexes I and II transfer electrons from NADH or FADH<sub>2</sub> onto ubiquinone, which is believed to freely diffuse within the inner mitochondrial membrane. Complex III transfers electrons from ubiquinol to cytochrome *c*. This small protein is localized in the space between the outer and inner mitochondrial membrane. Finally, complex IV transfers electrons from cytochrome *c* onto molecular oxygen. Three of the four oxidoreductase complexes couple electron transport with translocation of protons from the mitochondrial matrix to the intermembrane space. The generated proton gradient can be used by complex V to catalyze the formation of ATP by the phosphorylation of ADP. In plants and many fungi and protozoans, additional so-called “alternative” oxidoreductases occur (1, 2). Some of them can substitute complex I (alternative NADH dehydrogenases), others the complexes III and IV (alternative oxidases). In general, the alternative oxidoreductases do not couple electron transport with proton translocation across the inner mitochondrial membrane. These enzymes are considered to form the basis of an overflow protection mechanism for the respiratory chain under certain physiological conditions, *e.g.* high light conditions in plants.

\* This minireview will be reprinted in the 2007 Minireview Compendium, which will be available in January, 2008. This work was supported by the Deutsche Forschungsgemeinschaft and the Dutch Science Foundation NWO-CW.

<sup>1</sup> To whom correspondence should be addressed. E-mail: braun@genetik.uni-hannover.de.

<sup>2</sup> The abbreviations used are: OXPHOS, oxidative phosphorylation; EM, electron microscopy.

The structures of complexes II, III, and IV are known in great detail because of x-ray crystallography analyses (reviewed in Rich (3)). Also, parts of complexes I and V were resolved by this experimental strategy (4, 5). Complex II is the smallest oxidoreductase comprising only 4–8 different protein subunits (6, 7). The complexes III, IV, and V include 10–20 subunits, and complex I includes 40–50 different polypeptides (8–10). Electron transfer is mediated by a number of prosthetic groups and co-factors attached to defined subunits of the four oxidoreductase complexes: 2Fe-2S clusters, 4Fe-4S clusters, heme groups of the a, b, and c type, a flavine mononucleotide, and copper atoms. Many other subunits of the oxidoreductases are not directly involved in electron transfer but partially integrate side activities into the OXPHOS complexes. For instance, mitochondrial fatty acid biosynthesis takes place at an acyl carrier protein integrated into complex I (11, 12). Furthermore, a mitochondrial processing peptidase is integrated into complex III and carbonic anhydrases into complex I in plants (13, 14).

## Fluid State Versus Solid State Model

Despite the detailed knowledge on the structure of the individual OXPHOS complexes of the respiratory chain, their supramolecular organization is still largely unknown. Two extreme models were proposed, the “fluid state” and the “solid state” model (reviewed in Rich (15) and Lenaz (16)). According to the fluid state model, complexes I to IV diffuse freely in the inner mitochondrial membrane, and electron transfer is based on random collisions of the involved components. This model is supported by the fact that all five complexes can be purified in a physiologically active form and by lipid dilution experiments using isolated mitochondrial membranes (reviewed in Hackenbrock *et al.* (17)). In contrast, several other lines of evidence rather support the solid state model: (i) many isolation procedures for OXPHOS complexes result in the co-purification of more than one oxidoreductase (18), (ii) reconstitution experiments reveal highest electron transfer activities if different OXPHOS complexes are present at defined stoichiometries (19), (iii) point mutations within genes encoding subunits of one OXPHOS complex affect the stability of other OXPHOS complexes (20), (iv) flux control experiments indicate functional units larger than the single OXPHOS complexes (21, 22), (v) supercomplexes including more than one type of OXPHOS complex are displayed by native gel electrophoresis procedures or sucrose gradient centrifugation (23, 24), and (vi) analyses by single particle electron microscopy prove very defined associations of different OXPHOS complexes within respiratory supercomplexes (25, 26).<sup>3</sup> Using similar experimental approaches, respiratory supercomplexes also were reported for several bacteria (28, 29). Although there is still some debate on the membrane state of the OXPHOS system (for a recent discussion see Heinemeyer *et al.* (30)), it meanwhile is clear that the fluid state model cannot explain many experimental observations. However, interac-

<sup>3</sup> J. Heinemeyer, H. P. Braun, E. J. Boekema, and R. Kouril, submitted for publication.

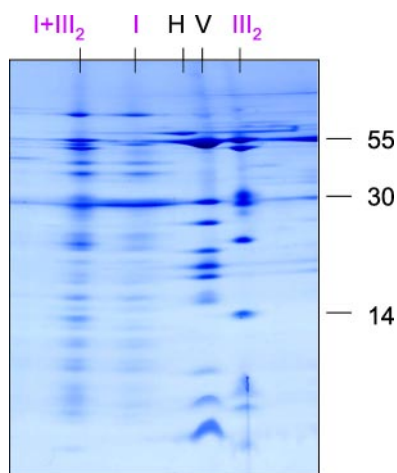


**FIGURE 1. Characterization of the I+III<sub>2</sub> supercomplex of *Arabidopsis* by native gel electrophoresis.** Mitochondrial membranes were solubilized by 5% digitonin, and proteins were resolved by two-dimensional Blue-native SDS-PAGE. Proteins were visualized by Coomassie staining. Molecular masses of standard proteins are given to the right, designations of resolved protein complexes are given above the two-dimensional gel (in kDa). *H*, HSP60 complex.

tions of OXPHOS complexes also are not simply “solid” but rather should be considered to be of a dynamic nature. In the following sections we review new insights into mitochondrial OXPHOS supercomplex structure and function.

### Structure of OXPHOS Supercomplexes

Starting point for structural characterization of respiratory supercomplexes is their solubilization using non-ionic detergents. This step appears to be very critical. The classical detergents Triton X-100 and digitonin were found to be the most suitable ones to obtain a variety of stable supercomplexes (23). Solubilization can be nicely monitored by Blue-native PAGE, a procedure that employs Coomassie dyes to introduce negative charge into proteins and protein complexes before electrophoretic separation (31). If combined with SDS-PAGE, supercomplexes are resolved into their subunits (Fig. 1). Many OXPHOS supercomplexes were first identified and characterized using this experimental strategy: (i) dimeric ATP synthase, (ii) a “I+III<sub>2</sub> supercomplex” including complex I and dimeric complex III, (iii) “III<sub>2</sub>+IV<sub>1-2</sub> supercomplexes” consisting of dimeric complex III and one or two copies of monomeric complex IV, and (iv) very large “I+III<sub>2</sub>+IV<sub>1-4</sub> supercomplexes” comprising complexes I, dimeric complex III, and one to four copies of complex IV (23, 24, 32–34). These supercomplexes were described for a broad range of organisms including fungi, mammals, plants, and algae. However, abundance and stability of the OXPHOS supercomplexes vary among different organisms. Dimeric ATP synthase proved to be especially stable in the algae *Chlamydomonas* and *Polytomella*, the I+III<sub>2</sub> supercomplex in *Arabidopsis*, the III<sub>2</sub>+IV<sub>1-2</sub> complexes in yeast, and the I+III<sub>2</sub>+IV<sub>1-4</sub> supercomplexes in beef. These comparatively stable supercomplexes were selected for further investigation using single particle electron microscopy (EM). For the preparation of supercomplexes prior to EM analyses, Blue-native PAGE usually is substituted by sucrose gradient ultracentrifugation.

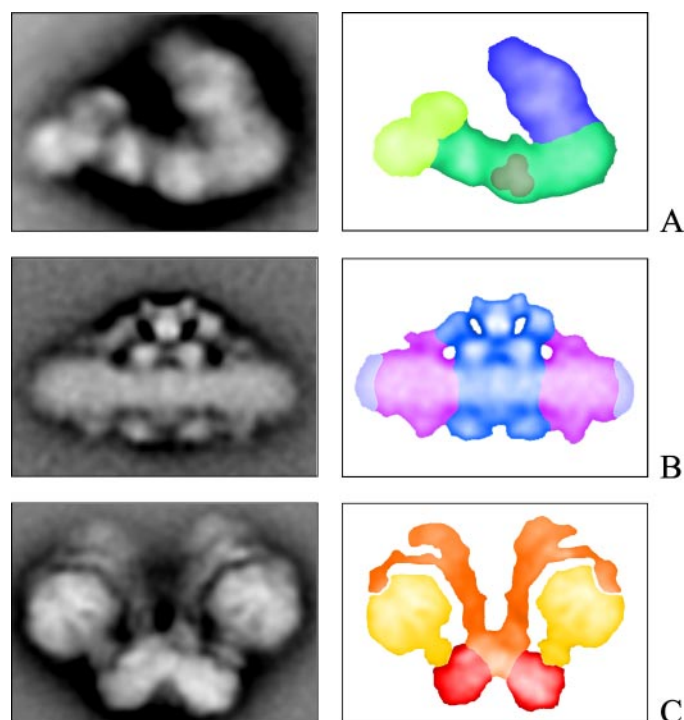


**FIGURE 2. Structure of mitochondrial OXPHOS supercomplexes as revealed by single particle electron microscopy.** *A*, top view projection map of the I+III<sub>2</sub> supercomplex of *Arabidopsis* (25); *B*, side view map of the III<sub>2</sub>+IV<sub>2</sub> supercomplex of yeast<sup>3</sup>; *C*, side view map of dimeric ATP synthase of *Polytomella* (39). In the schemes protein complexes or large protein domains are indicated by colors. *A*: complex III<sub>2</sub>, blue; complex I, green (light green, peripheral arm; medium green, membrane arm; dark green, carbonic anhydrase domain). *B*: complex III<sub>2</sub>, blue; complex IV, purple. *C*: F<sub>0</sub> parts, red; F<sub>1</sub> parts and central stalks, yellow; peripheral stalks, orange.

*The I+III<sub>2</sub> Supercomplex*—This supercomplex was the first OXPHOS supercomplex to be structurally analyzed (25). It so far is only characterized for *Arabidopsis* (Fig. 2*A*). Single particle EM projections turned out to mainly represent “top views” of the I+III<sub>2</sub> supercomplex (perspective from the mitochondrial matrix). Two-dimensional maps revealed a lateral association of dimeric complex III (blue on Fig. 2*A*) to the membrane arm of complex I (medium green) within the inner mitochondrial membrane. The peripheral arm of complex I (light green) protrudes out of the plane of the image. The membrane arm of complex I is bent around dimeric complex III at the site of interaction. Compared with mammalian mitochondria, this arm is slightly longer in *Arabidopsis*. This possibly explains the special stability of the I+III<sub>2</sub> supercomplex in this organism. It currently is not precisely known which subunits are localized at the complex I-complex III interface.

*The III<sub>2</sub>+IV<sub>1-2</sub> Supercomplexes*—A first structural model of this supercomplex was recently resolved for yeast.<sup>3</sup> In the obtained projection maps the supercomplex is seen in different side view positions (Fig. 2*B*). A view along the longest axis through the supercomplex reveals that two complex IV monomers (purple on Fig. 2*B*) are associated to the central complex III dimer (blue). The Cox I, II, IV, and VIIc subunits on the complex IV side and the cytochrome *c*<sub>1</sub>, hinge, VII, and VIII subunits on the complex III side are predicted to be localized at the complex IV-III<sub>2</sub> interface. Some other projection maps indicate that the III<sub>2</sub>+IV<sub>1</sub> supercomplex has the same structure

but just lacks one complex IV monomer. Other complexes include one or two copies of cytochrome *c* attached to the supercomplex at a location predicted from earlier x-ray crystallography studies (35).

**The  $I+III_2+IV_{1-4}$  Supercomplexes**—These supercomplexes represent the largest forms of OXPHOS complex assemblies and also are termed “respirasomes” (23). First insights into the architecture of respirasomes were recently reported for beef (26). Projection maps showing the  $I+III_2+IV_1$  supercomplex within the membrane plane revealed the position of complexes I and  $III_2$ . As within the  $I+III_2$  supercomplex of *Arabidopsis*, dimeric complex III is laterally bound to the membrane arm of complex I. According to a presented model, complex IV is attached to the tip of the membrane arm of complex I but at the same time laterally interacts with the complex III dimer. However, due to limited resolution, other interpretations currently cannot be fully excluded. Also, the subunits localized at the interfaces between the complexes I,  $III_2$ , and IV are so far unknown.

**Dimeric ATP Synthase**—Dimeric ATP synthase was first described for yeast (32). The supercomplex includes three dimer-specific proteins termed subunits e, g, and k. Interestingly, deletion of the gene encoding subunit g not only disturbs dimerization of ATP synthase but also drastically changes mitochondrial ultrastructure. In the mutants, mitochondria are much enlarged, and the inner mitochondrial membrane is devoid of its characteristic folding pattern termed cristae (36, 37). It therefore was speculated that dimerization of ATP synthase is important for cristae formation. A similar ultrastructural phenotype was obtained upon *in vivo* cross-linking of the  $F_1$  domains of ATP synthase in yeast (38). The EM structure of dimeric ATP synthase from beef, yeast, and *Polytomella* indeed supports a role of ATP synthase dimerization in cristae formation because interaction of the ATP synthase monomers was found to cause a local bend of the inner mitochondrial membrane (39–41). Highest resolution was obtained for the structure of dimeric ATP synthase of *Polytomella* (Fig. 2C). Projection maps of dimers in the side view position reveal that the monomers exclusively interact in the region of the membrane-bound  $F_0$  domains (red on Fig. 2C) and that the angle between the long axes of the two monomers is about 70°. In contrast, this angle was found to be 40° in beef and approximately either 40° or 90° in yeast. Investigations by Blue-native PAGE indicate occurrence of even larger ATP synthase assemblies (36, 42, 43), which so far could not be analyzed by single particle EM. However, long double rows of particles were described by rapid freeze-deep etch EM and interpreted as large numbers of laterally attached ATP synthase dimers (44, 45). These structures are speculated to be important for the formation of tubular invaginations of the inner mitochondrial membrane. The two classes of angles between ATP synthase monomers obtained by single particle EM, wide range (70–90°) and narrow range (~40°), possibly represent different forms of monomer interactions (transverse or longitudinal) within the ATP synthase oligomers (41).

### Function of OXPHOS Supercomplexes

The supramolecular organization of the OXPHOS system is considered to be of great functional importance. Respiratory

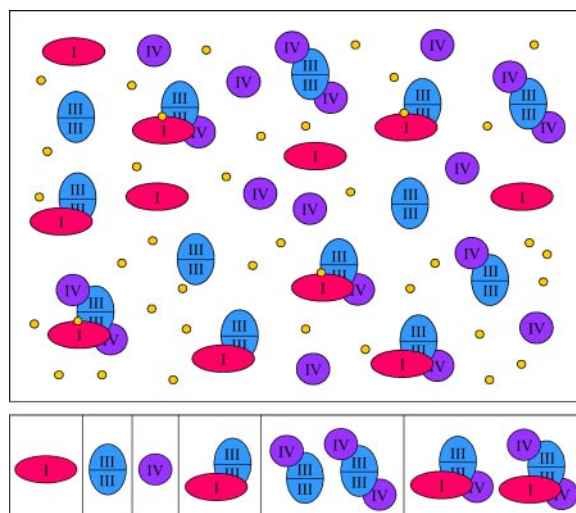


**FIGURE 3. Model of the supramolecular structure of the OXPHOS system: single complexes co-exist with supramolecular assemblies.** Complex I (red) can associate with complex  $III_2$  (blue). Complex  $III_2$  can associate with one or two copies of complex IV (purple). The largest assemblies include complex I, dimeric complex III, and one or several copies of complex IV. Yellow circles, ubiquinol, which either freely diffuses within the inner mitochondrial membrane or might form part of the  $I+III_2$  supercomplex. For simplicity, complex II was omitted from the figure because it is not known to form part of OXPHOS supercomplexes. Furthermore, cytochrome *c*, alternative oxidoreductases, and the ATP synthase complex are omitted from the figure. Modified from Bianchi *et al.* (27).

supercomplexes may (i) allow enhanced electron transfer rates (electron channeling), (ii) represent regulatory units of respiration, (iii) determine the ultrastructure of the inner mitochondrial membrane, (iv) increase the stability of OXPHOS complexes, and (v) increase the protein insertion capacity of the inner mitochondrial membrane. Several experimental observations confirm one or the other roles of the OXPHOS supercomplexes. Determination of cristae structure might not only be a function of ATP synthase dimers but possibly also of other OXPHOS supercomplexes. However, based on the single particle EM structures obtained, membrane bending by supercomplexes comprising complexes I–IV is less obvious. Enhanced electron transfer rates of the  $I+III_2$  supercomplex compared with a mixture of singular complex I and  $III_2$  were measured under *in vitro* conditions (23). Nevertheless, direct electron channeling possibly does not occur because the predicted ubiquinol reduction site at complex I and the ubiquinol oxidation site at complex  $III_2$  are not in close proximity within the single particle structure obtained for this supercomplex. In contrast, electron channeling is likely to occur in the  $III_2+IV_{2-1}$  supercomplexes. The cytochrome *c* binding sites of the complexes III and IV are in close proximity.<sup>3</sup> Also, EM projection maps partially include bound cytochrome *c* at the predicted position (35). Alternate stabilization of OXPHOS complexes within supercomplexes is supported by the characterization of OXPHOS mutants (20).

There are many indications that OXPHOS complexes do not always form part of OXPHOS supercomplexes. This can be deduced simply by the differing concentrations of the individual OXPHOS complexes within the inner mitochondrial membrane. Most likely, single and associated OXPHOS complexes co-exist within the inner mitochondrial membrane (Fig. 3).

Their ratio is speculated to be regulated by so far unknown factors. One of these factors might be the lipid cardiolipin (46–48).

### Perspectives

The functional roles of OXPPOS supercomplexes have to be further investigated. Obviously, high resolution structures based on single particle cryo-EM or x-ray crystallography will represent a basis to better understand supercomplex function. Furthermore, non-invasive methods to analyze the supramolecular structure of the OXPPOS system are very important to finally exclude that artificial aggregations are generated during disruption of mitochondrial membranes. However, there are currently no indications that the detergents used for OXPPOS supercomplex characterizations produce any artifacts. Also, evidence for the occurrence of OXPPOS supercomplexes is based very heavily on detergent-free experimental strategies like rapid freeze-deep etch EM, flux control measurements, and the characterization of mutants. Future research on the supramolecular structure of the OXPPOS system should be based on a broad scale of different procedures, including cryo-EM tomography, atomic force microscopy in aqueous solution, and other newly developed experimental systems. This will be especially important for the investigation of even larger “string”-like hyperstructures of the OXPPOS system, which are proposed to exist under *in vivo* conditions (49).

### REFERENCES

- Vanlerberghe, G. C., and McIntosh, L. (1997) *Annu. Rev. Plant Physiol. Plant Mol. Biol.* **48**, 703–734
- Rasmusson, A. G., Soole, K. L., and Elthon, T. E. (2004) *Annu. Rev. Plant Biol.* **55**, 23–39
- Rich, P. R. (2003) *Biochem. Soc. Trans.* **31**, 1095–1105
- Sazanov, L. A., and Hinchliffe, P. (2006) *Science* **311**, 1430–1436
- Dickson, V. K., Silvester, J. A., Fearnley, I. M., Leslie, A. G., and Walker, J. E. (2006) *EMBO J.* **25**, 2911–2918
- Horsefield, R., Iwata, S., and Byrne, B. (2004) *Curr. Protein Pept. Sci.* **5**, 107–118
- Millar, A. H., Eubel, H., Jansch, L., Kruft, V., Heazlewood, J. L., Braun, H. P. (2004) *Plant Mol. Biol.* **56**, 77–89
- Berry, E. A., Guergova-Kuras, M., Huang, L. S., and Crofts, A. R. (2000) *Annu. Rev. Biochem.* **69**, 1005–1075
- Richter, O. M. H., and Ludwig, B. (2003) *Rev. Physiol. Biochem. Pharmacol.* **147**, 47–74
- Brandt, U. (2006) *Annu. Rev. Biochem.* **75**, 69–92
- Runswick, M. J., Fearnley, I. M., Skehel, J. M., and Walker, J. E. (1991) *FEBS Lett.* **286**, 121–124
- Sackmann, U., Zensen, R., Röhlen, D., Jahnke, U., and Weiss, H. (1991) *Eur. J. Biochem.* **200**, 463–469
- Braun, H. P., Emmermann, M., Kruft, V., and Schmitz, U. K. (1992) *EMBO J.* **11**, 3219–3227
- Sunderhaus, S., Dudkina, N. V., Jansch, L., Klodmann, J., Heinemeyer, J., Perales, M., Zabaleta, E., Boekema, E. J., and Braun, H. P. (2006) *J. Biol. Chem.* **281**, 6482–6488
- Rich, P. R. (1984) *Biochim. Biophys. Acta* **768**, 53–79
- Lenaz, G. (2001) *FEBS Lett.* **509**, 151–155
- Hackenbrock, C. R., Chazotte, B., and Gupta, S. S. (1986) *J. Bioenerg. Biomembr.* **18**, 331–368
- Hatefi, Y., and Rieske, J. S. (1967) *Methods Enzymol.* **10**, 225–231
- Ragan, C. I., and Heron, C. (1978) *Biochem. J.* **174**, 783–790
- Acin-Perez, R., Bayona-Bafaluy, M. P., Fernandez-Silva, P., Moreno-Loshuertos, R., Perez-Martos, A., Bruno, C., Moraes, C. T., and Enriquez, J. A. (2004) *Mol. Cell* **13**, 805–815
- Boumans, H., Grivell, L. A., and Berden, J. A. (1998) *J. Biol. Chem.* **273**, 4872–4877
- Bianchi, C., Genova M. L., Castelli, G., and Lenaz, G. (2004) *J. Biol. Chem.* **279**, 36562–36569
- Schägger, H., and Pfeiffer, K. (2000) *EMBO J.* **19**, 1777–1783
- Eubel, H., Jansch, L., and Braun, H. P. (2003) *Plant Physiol.* **133**, 274–286
- Dudkina, N. V., Eubel, H., Keegstra, W., Boekema, E. J., and Braun, H. P. (2005) *Proc. Natl. Acad. Sci. U. S. A.* **102**, 3225–3229
- Schäfer, E., Seelert, H., Reifschneider, N. H., Krause, F., Dencher, N. A., and Vonck, J. (2006) *J. Biol. Chem.* **281**, 15370–15375
- Bianchi, C., Fato, R., Genova, M. L., Castelli, G. P., and Lenaz, G. (2003) *Biofactors* **18**, 3–9
- Berry, E. A., and Trumpower, B. L. (1985) *J. Biol. Chem.* **260**, 2458–2467
- Stroh, A., Anderka, O., Pfeiffer, K., Yagi, T., Finel, M., Ludwig, B., and Schägger, H. (2004) *J. Biol. Chem.* **279**, 5000–5007
- Heinemeyer, J., Dudkina, N. V., Boekema, E. J., and Braun, H. P. (2007) in *Plant Mitochondria* (Logan, D. C., ed) Blackwell Publishing, Oxford, UK, in press
- Schägger, H., and von Jagow, G. (1991) *Anal. Biochem.* **199**, 223–231
- Arnold, I., Pfeiffer, K., Neupert, W., Stuart, R. A., and Schägger, H. (1998) *EMBO J.* **17**, 7170–7178
- Krause, F., Scheckhuber, C. Q., Werner, A., Rexroth, S., Reifschneider, N. H., Dencher, N. A., and Osiewacz, H. D. (2003) *J. Biol. Chem.* **279**, 26453–26461
- Van Lis, R., Atteia, A., Mendoza-Hernandez, G., and Gonzalez-Halphen, D. (2003) *Plant Physiol.* **132**, 318–330
- Lange, C., and Hunte, C. (2002) *Proc. Natl. Acad. Sci. U. S. A.* **99**, 2800–2805
- Paumard, P., Vaillier, J., Coulary, B., Schaeffer, J., Soubannier, V., Mueller, D. M., Brethes, D., di Rago, J. P., and Velours, J. (2002) *EMBO J.* **21**, 221–230
- Giraud, M. F., Paumard, P., Soubannier, V., Vaillier, J., Arselin, G., Salin, B., Schaeffer, J., Brèthes, D., di Rago, P., and Velours, J. (2002) *Biochim. Biophys. Acta* **1555**, 174–180
- Gavin, P. D., Prescott, M., Luff, S. E., and Devenish, R. J. (2004) *J. Cell Sci.* **117**, 2233–2243
- Minauro-Sanmiguel, F., Wilkens, S., and Garcia, J. J. (2005) *Proc. Natl. Acad. Sci. U. S. A.* **102**, 12356–12358
- Dudkina, N. V., Heinemeyer, J., Keegstra, W., Boekema, E. J., and Braun, H. P. (2005) *FEBS Lett.* **579**, 5769–5772
- Dudkina, N. V., Sunderhaus, S., Braun, H. P., and Boekema, E. J. (2006) *FEBS Lett.* **580**, 3427–3432
- Krause, F., Reifschneider, N. F., Goto, S., and Dencher, N. A. (2005) *Biochem. Biophys. Res. Commun.* **329**, 583–590
- Wittig, I., and Schägger, H. (2005) *Proteomics* **5**, 4338–4346
- Allen, R. D., Schroeder, C. C., and Fok, A. K. (1989) *J. Cell Biol.* **108**, 2233–2240
- Allen, R. D. (1995) *Protoplasma* **189**, 1–8
- Zhang, M., Mileykovskaya, E., and Dowhan, W. (2002) *J. Biol. Chem.* **277**, 43553–43556
- Pfeiffer, K., Gohil, V., Stuart, R. A., Hunte, C., Brandt, U., Greenberg, M. L., and Schägger, H. (2003) *J. Biol. Chem.* **278**, 52873–52880
- Zhang, M., Mileykovskaya, E., and Dowhan, W. (2005) *J. Biol. Chem.* **280**, 29403–29408
- Wittig, I., Carrozzo, R., Santorelli, F. M., and Schägger, H. (2006) *Biochim. Biophys. Acta* **1757**, 1066–1072